CHAPTER III

EXPERIMENTAL DETAILS

In this chapter, the sample fabrication processes by droplet epitaxy technique are described in details. The growth equipment, molecular beam epitaxy (MBE), is introduced. In situ reflection high-electron energy diffraction (RHEED) installed with this MBE system is used to calibrate the growth rate and observe the evolution of surface structure during the growth. Also, ex situ characterizing-techniques including atomic force microscopy (AFM) and photoluminescence (PL) spectroscopy are introduced.

3.1 Molecular Beam Epitaxy

Molecular beam epitaxy (MBE) is a popular technique for growing III-V compound semiconductors. With a clean and ultra high vacuum (UHV) environment, the molecular beams of the constituent elements are incident upon a heated crystalline substrate and produce high-quality layers with very abrupt interfaces. It also has good control of thickness, doping, and composition, because of very low growth rate (monolayer (ML)/s), and the precise control of beam fluxes and growth conditions on an atomic scale. Quantum devices with high efficiency, high speed and high performance can be demonstrated. It can be said that MBE-grown quantum well structures closely approximate the idealized square-well potential models used in solid state theory.

In this research, a solid-source conventional RIBER 32P MBE machine consisting of three UHV chamber modules, i.e., introduction chamber, transfer chamber, and growth chamber, is used to fabricate the samples. Three chambers are separated by isolation gate valves. The pumping system including ion pumps, and titanium sublimation pumps are installed to keep UHV condition. A figure of RIBER 32P MBE is shown in Figure 3.1. The pressure of each chamber is measured by an ionization gauge. Epitaxial growth is done in the growth chamber cooled by liquid N_2 to keep base pressure below ~ 1×10^{-10} Torr. The manipulator with the substrate is rotated continuously during the growth to provide a uniform flux profile on the substrate

surface. The group III-elements (i.e. In, Ga, and Al) and group V-elements (i.e. As_4) are contained in pyrolytic boron nitride (PBN) crucibles which are installed in a separated effusion cells. Each cell is heated by its own heater the temperature of which is controlled by feedback from a standard thermocouple to a computer. The molecular beam flux of each element is controlled by a tantalum shutter in the front of each cell. A schematic drawing of the modified III-V MBE growth chamber is shown in Figure 3.2.

The unique advantage of MBE from other techniques is to study and control the growth process in situ. In particular, reflection high energy electron diffraction (RHEED) allows directly monitoring the surface structure of the sample and the already grown epilayer. The explanation on RHEED is presented in the next section. In addition, quadrapole mass spectroscopy is also used for particle analysis in the growth chamber.

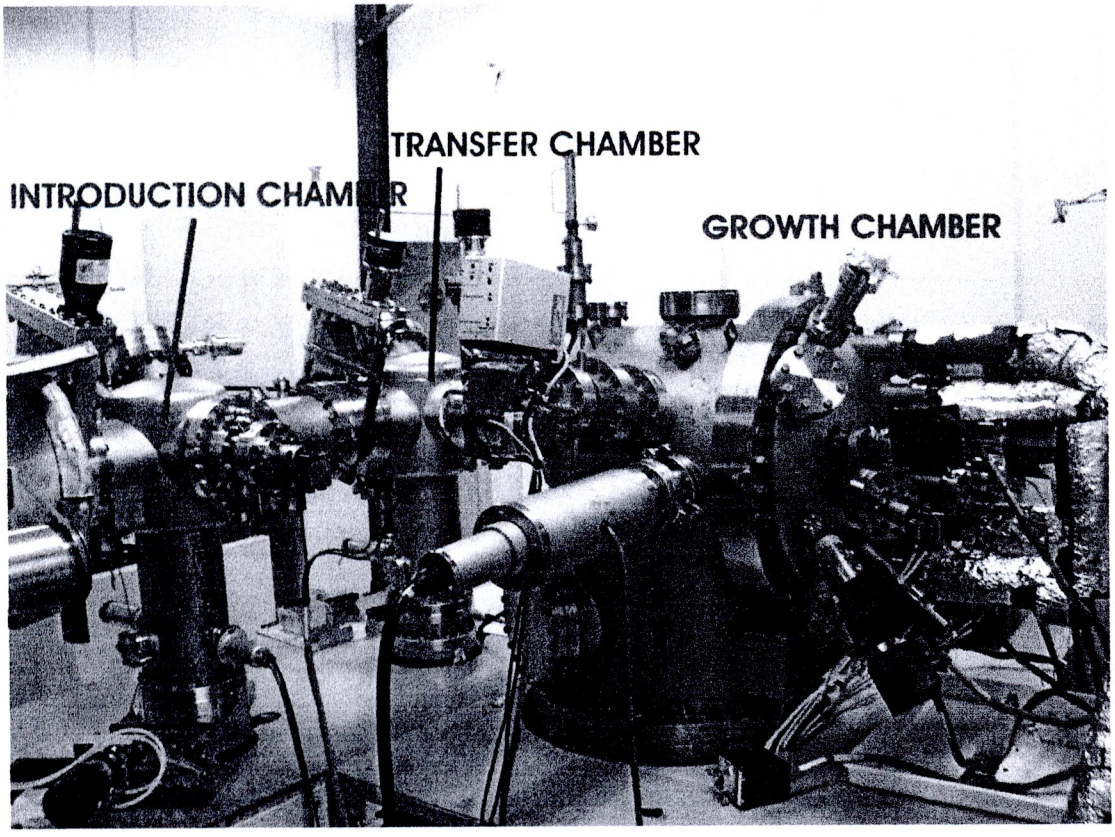

Figure 3.1 The conventional RIBER 32P MBE.

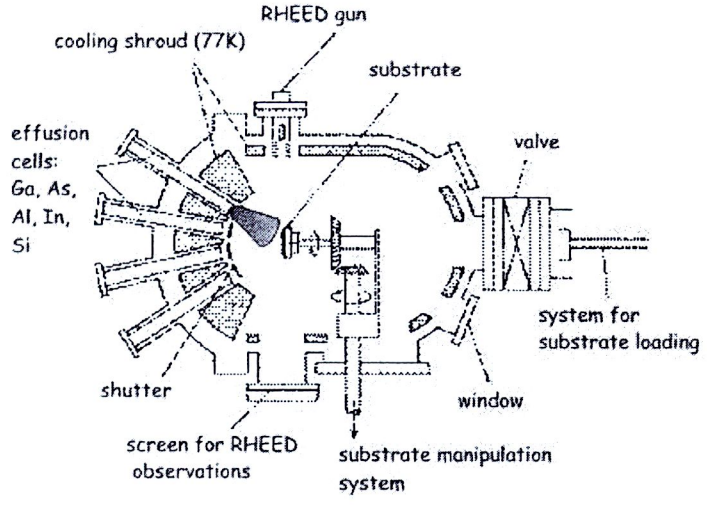

Figure 3.2 Schematic drawing of the modified III-V MBE growth chamber. The chamber is cooled by liquid N_2 (the base pressure < 1×10^{-10} torr).

3.2 Reflection High Energy Electron Diffraction (RHEED)

Reflection high energy electron diffraction is an in situ technique for characterizing thin films. It allows direct monitoring of the surface structure of the sample and already grown epilayer. It also allows observation on the dynamics of the growth. A schematic representation of a RHEED system is shown in Figure 3.3. A high-energy electron beam (~15 keV) intersects with the sample surface at a small angle (θ ~1-3°). It is diffracted by the surface atoms, which function as a grating. The scattered electrons interfere constructively and form a pattern on the fluorescent screen. The RHEED pattern is captured with a high-performance CCD camera and analyzed by the data processing software installed in the computer.

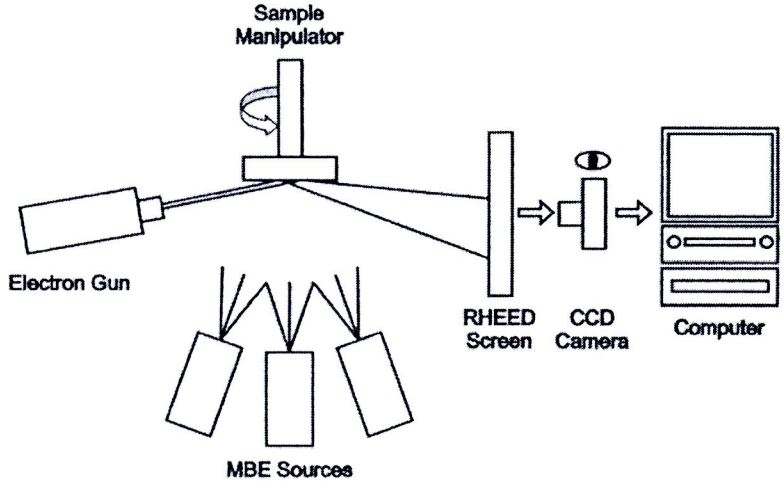

Figure 3.3 Schematic representation of RHEED system.

The pattern position can be graphically determined by the Laue method – intersection of Edwald sphere in the reciprocal lattice space. A schematic representation of RHEED observation is illustrated in Figure 3.4. Since the short de Broglie wavelength of electrons allows a shallow penetration depth into the substrate, the electron beam samples the topmost atomic layers. The diffracted electrons at the flat surface are imaged onto the screen. Therefore, the surface layer is represented by a reciprocal lattice space rod perpendicular to the real surface [44]. If the surface has roughness in the order of an atomic scale, the surface layer in the reciprocal space will be presented by three-dimensional point array. Therefore, we can interpret the RHEED pattern as the reciprocal lattice representation of the sample surface, which reflects the surface morphology on the atomic scale.

In this work, in situ RHEED observation is used to monitor surface structures during the growth of GaAs buffer layer and during the growth of nanostructures.

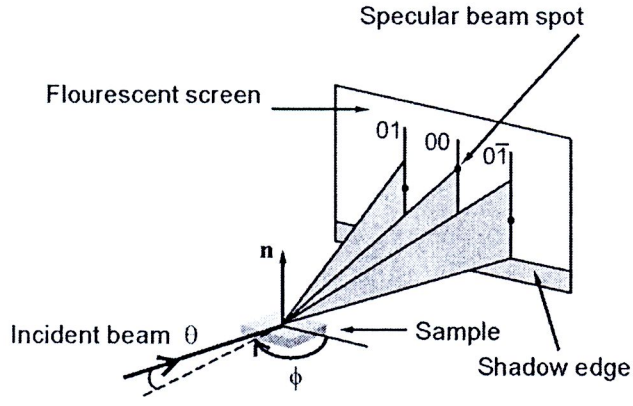

Figure 3.4 Schematic diagram of RHEED geometry of the incident electron beam at an angle θ to the surface plane [44].

3.2.1 RHEED intensity oscillation

The growth rates also can be determined by using RHEED intensity oscillations. The intensity oscillations are used to calibrate group III beam fluxes corresponding to the growth rate. To control the alloy composition and the thickness of quantum structures grown, the fluxes are adjusted to the value corresponding to needed growth rate [44].

The RHEED intensity on the pattern depends on the roughness of the surface. Under the normal growth conditions, the RHEED intensity, i.e., surface roughness, changes according to the fraction of surface coverage where a period of the pattern oscillation corresponds to the growth of 1 monolayer (ML). A schematic representation of the RHEED intensity oscillations is shown in Figure 3.5. In each period, the maximum reflectivity occurs at the initial and final state with a completed smooth surface and the minimum reflectivity occurs at the intermediate state when the grown layer is approximately half completed. With use of the period of oscillation signal, the growth rate of GaAs and others can be calibrated too.

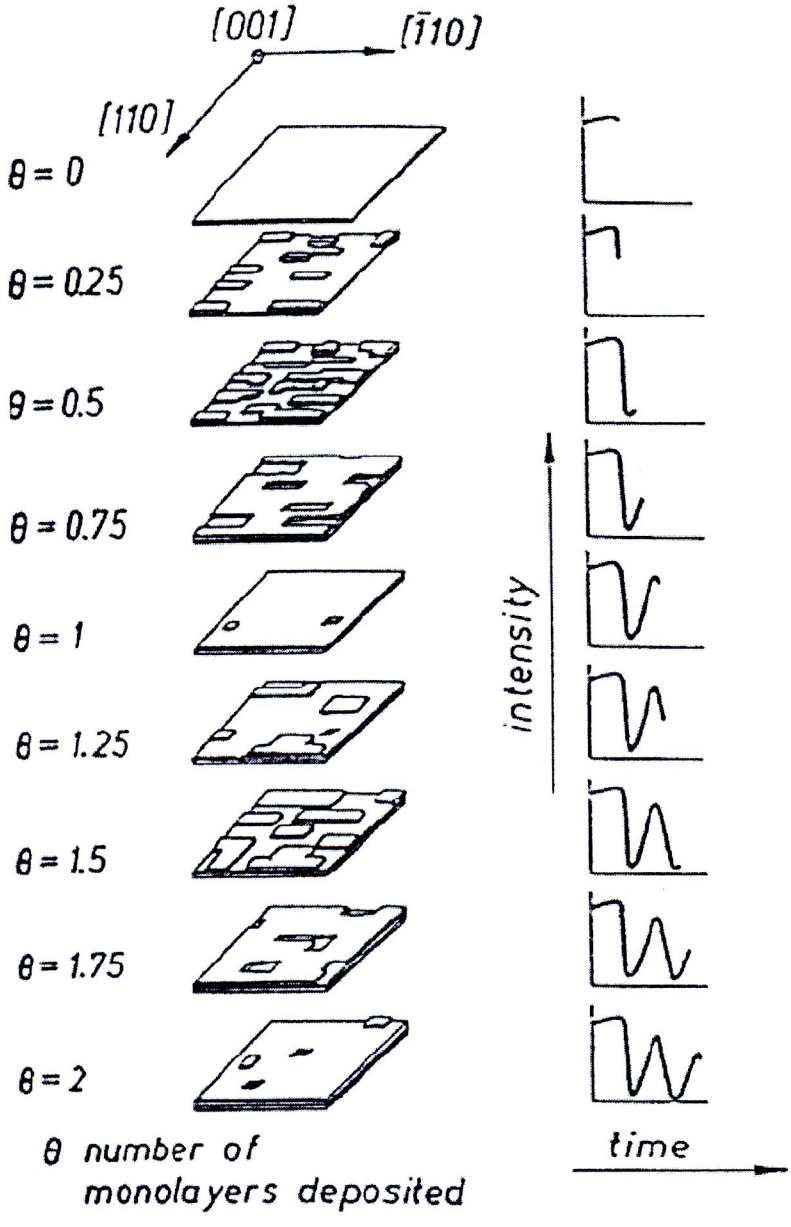

Figure 3.5 Schematic representation of RHEED intensity oscillations related to formation of the first two completed monolayer of GaAs (001) [44].

3.3 Atomic Force Microscopy (AFM)

Atomic force microscopy (AFM) is a very powerful microscopic technique, a demonstrated resolution of fractions of a nanometer. A schematic representation of an AFM system is shown in Figure 3.6. The AFM scanning module consists of a cantilever

with a sharp silicon or silicon nitride tip, the size of which is in the order of nanometers at its end. The tip is brought into close proximity of a sample surface and scan through out the selected area. Typically, the deflection is measured by a laser spot reflected from the metal coated top of the cantilever into an array of photodiodes and digitally processed. A schematic representation of AFM measuring modes is shown in Figure 3.7. In this work, the AFM is operated in the tapping mode to reduce the friction during the measurement.

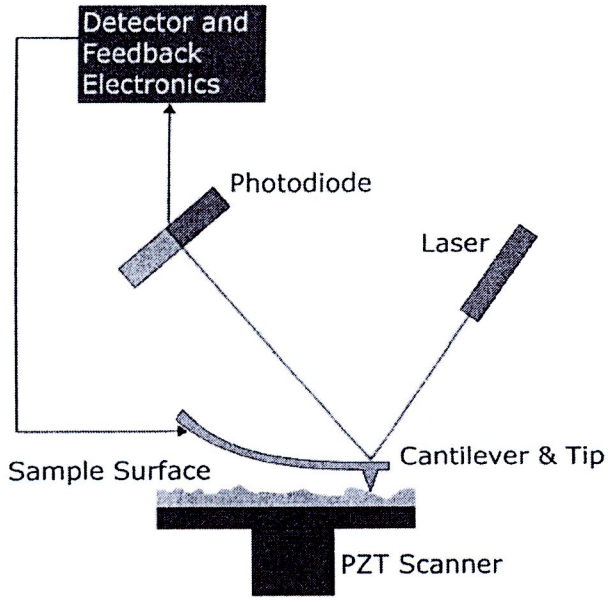

Figure 3.6 Schematic drawing of Atomic Force Microscopy (Drawn October 12, 2002 by Allen Timothy Chang).

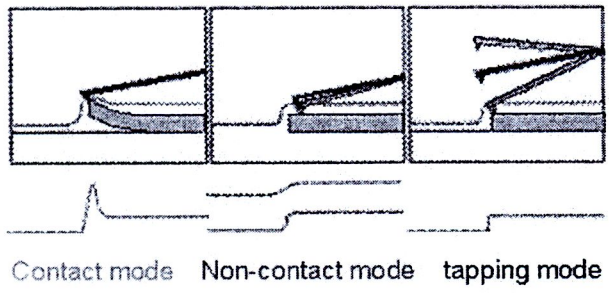

Figure 3.7 The schematic representation of AFM measuring modes including contact mode, non-contact mode and tapping mode.

In this work, the AFM images are performed by using a SEIKO SPA 400-AFM. The AFM is operated in the tapping mode in order to reduce the friction during the measurement. The scan rate is about 1-2 Hz (line per second) and the scan size is usually 1×1 - 5×5 μm^2 with 512 data points per scan line.

3.4 Photoluminescence (PL) Measurement

Photoluminescence (PL) spectroscopy is a technique for characterizing the optical properties of a sample through its luminescence. A schematic of the PL experimental setup is shown in Figure 3.8. The samples are excited by the 478-nm line of an Ar^+ laser. The laser beam is chopped and focused to the sample by focal lens. The light signal is analyzed by using a monochromator. A high-pass filter is used to filter the visible-light noise and the reflected laser beam signal. Then, the resolved light is detected by a liquid-Nitrogen-cooled InGaAs detector. A chopper and a lock-in amplifier are used to enhance the signal by the standard lock-in technique. The polarizer is installed to the system when we characterize the polarization of the QR systems.

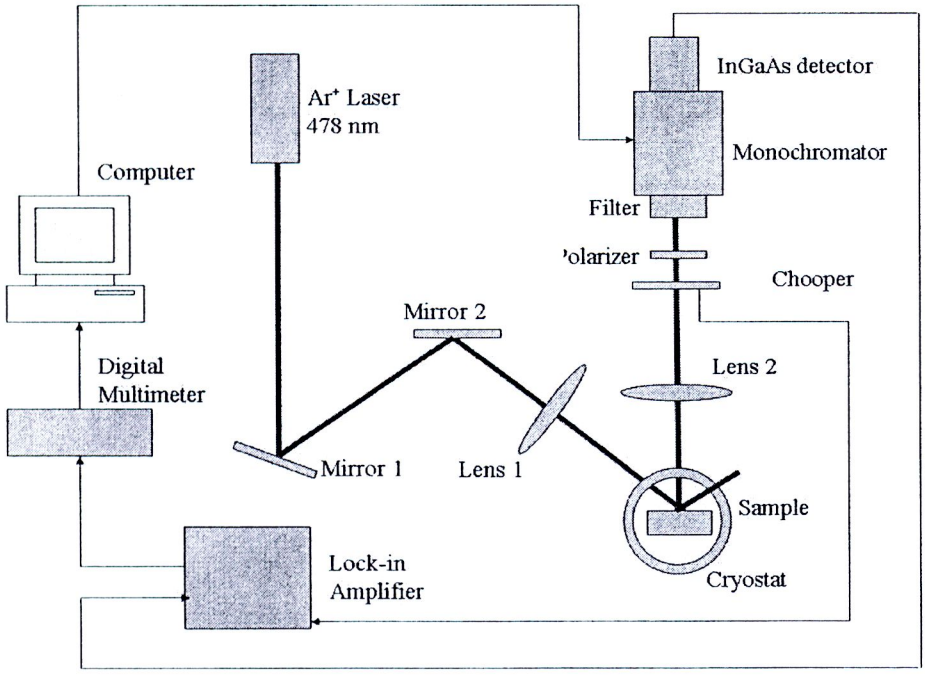

Figure 3.8 Schematic of the PL experimental setup

The PL result can provide the luminescence properties of a nanostructure system. In Figure 3.9, the ground state PL peak energy contains information about the size of the nanosturcture. The nanostructure with a larger size would have a lower quantized energy levels of both holes and electrons, which causes a lower PL peak energy position. Therefore, this PL peak position can be used to compare the size of nanostructures. In addition, the different size of nanostructures in an array can affect the shape of the PL spectrum as shown in Figure 3.10. A broadening of the spectrum, which is measured in terms of full width at half maximum (FWHM) or PL linewidth, is related to the nanostructure size distribution. Moreover, a polarization-resolved PL spectrum gives information on the nanostructure shape or nanostructure-system alignment in different crystal directions.

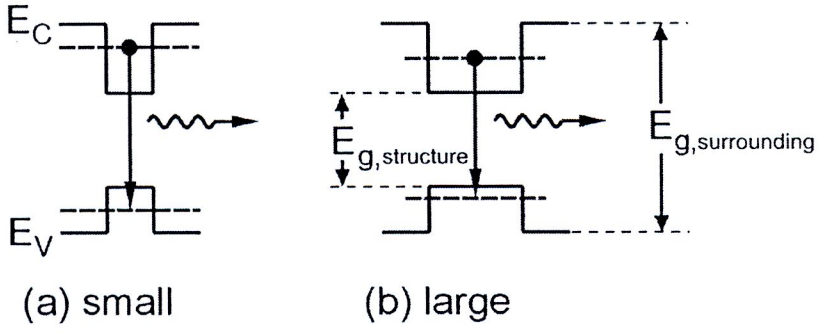

Figure 3.9 A simple interpretation of the PL data from a nanostructure; (a) higher PL peak energy position from a small-size nanostructure and (b) lower PL peak position from a large-size nanostructure.

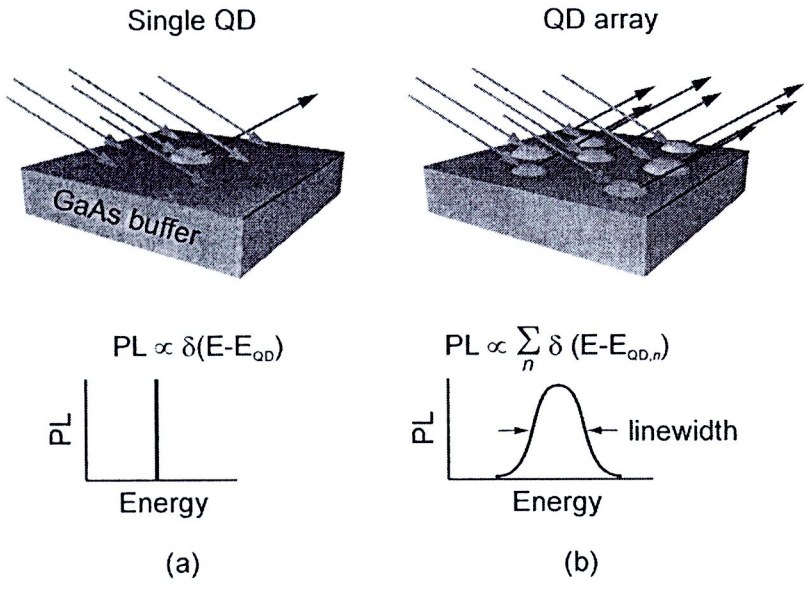

Figure 3.10 A comparative of the PL spectrum from a single QD and QD array; (a) narrow PL spectrum due to the delta-function like density of states of a QD. (b) The PL *peak* energy position and the PL *linewidth* interpreting the *average size* and the *size distribution* of the QD array, respectively.

3.5. Experimental Procedures

In this work, the samples of InGaAs QRs were fabricated on GaAs (100) substrates by droplet epitaxy using a RIBER 32P conventional solid-source MBE system. The growth conditions have been varied for droplet formation. A detailed sequence for sample preparation is as follows.

(1) Pre-heating: A piece of epi-ready semi-insulating (100) GaAs substrate was attached to a Mo (molybdenum) block (substrate holder) by indium glue. The block with the substrate was transferred to the introduction chamber and heated to 450°C for 60 minutes in order to eliminate water vapor and oxide from the substrate.

(2) Deoxidation: After pre-heating, the sample (the substrate mounted on a Mo block) was transferred into the UHV growth chamber. The native oxide of the GaAs substrate surface was removed by slowly ramping up to 600°C

under an As_4 flux of ~ 7×10^{-6} torr until a streaky RHEED showed a clear and abrupt pattern as shown in Figure 3.11.

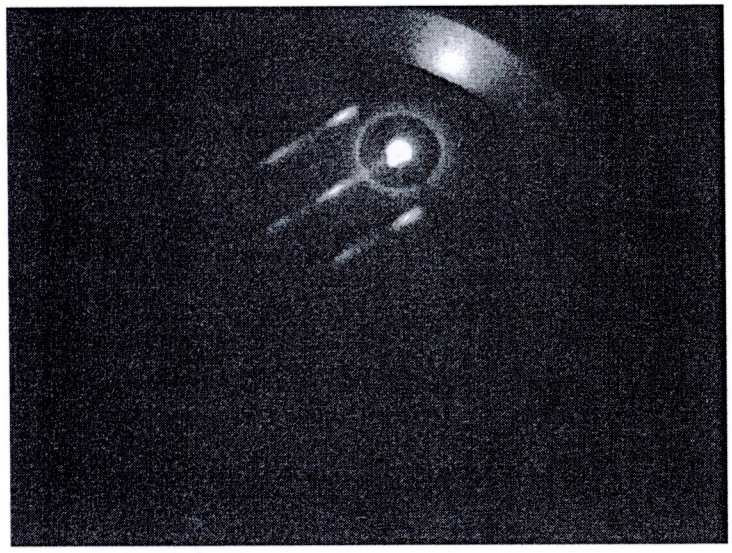

Figure 3.11 Streak RHEED pattern observed during the de-oxidation process.

(3) Growth of the GaAs buffer layer: a 300-nm thick undoped GaAs buffer layer was grown at 580°C to smooth the surface. The growth rate of GaAs was 1 monolayer/s (ML/s). A clear streaky (2×4) RHEED pattern was always observed after the growth of a buffer layer.

(4) Formation of InGa droplets: The growth conditions were varied in this step. First, the As_4 flux was turned off and the substrate temperature was lowered to 530°C to eliminate excess As atoms on the surface. Subsequently, the substrate temperature was decreased again to the desired deposition temperatures (T_s) in the absence of As_4. Then, the process was paused until the background pressure in the growth chamber was below 1 x 10^{-9} Torr to minimize the initial interaction between the InGa metal and background arsenic during droplet formation.

(4.1) to investigate the effect of T_s and deposited $In_{0.5}Ga_{0.5}$ amount on InGaAs QRs, 2-5 ML $In_{0.5}Ga_{0.5}$ (an equivalent amount of $In_{0.5}Ga_{0.5}As$ when

As_4 is supplied) was deposited at T_s = 120-300°C to form InGa droplets on GaAs layer. The deposition rate of $In_{0.5}Ga_{0.5}$ was 1 ML/s.

(4.2) to investigate the effect of Indium-mole-fraction (x), 3 ML In_xGa_{1-x} (x = 0.3 - 0.7) was deposited at T_s = 150°C to form InGa droplets. The deposition rate of In_xGa_{1-x} was 1 ML/s.

(5) Crystallization: After deposition, the substrate temperature was slowly ramped to 180°C within 11 min. Finally, the InGa droplets were exposed to 6-7×10^{-6} torr of As_4 flux at 180°C for 5 min to crystallize the metallic droplets into InGaAs QRs [6,23]. Note that crystallization was done at 180°C for all samples to prevent inter-diffusion of In atoms out of the droplets. A schematic illustration of the sample structure after crystallization is shown in Figure 3.12 (a). After the growth, the samples were taken out of the MBE system and examined for their surface morphology ex situ by atomic force microscopy (AFM: SEIKO SPA 4000) in tapping mode.

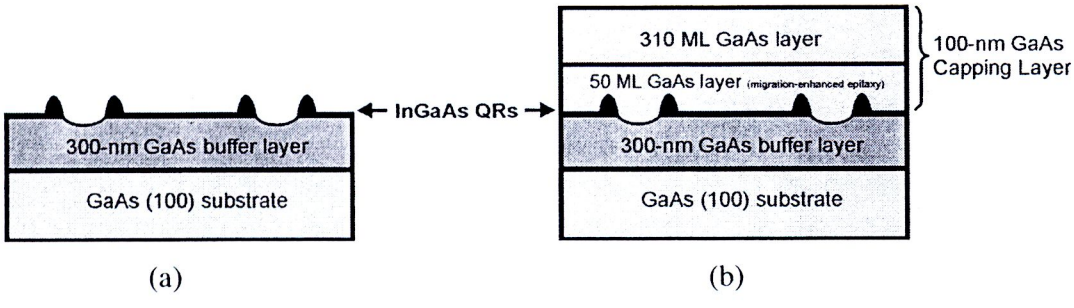

Figure 3.12 Schematic illustrations of the sample structures grown in this work (a) after crystallization in As_4, and (b) after capping with a 100-nm GaAs capping layer. The details of growth sequences and growth conditions for the InGaAs nanostructures are given in the text.

(6) GaAs capping (for PL measurement): another series of samples were grown under the conditions of 2-5 ML $In_{0.5}Ga_{0.5}$ deposition at T_s = 210°C with an additional 100-nm GaAs capping layer grown by the two-step growth method. After the entire growth sequences (1-5), the substrate temperature was slowly increased to 300°C in As_4 flux. Then, to prevent the deformation

of uncapped droplet-originated InGaAs QRs, the capping layer growth started with a 50-ML-thick GaAs grown by MEE at 300°C, by alternately supplying 50 cycles of Ga for 2 seconds (0.5 ML/s), As for 2 seconds and interrupting for 2 seconds [55,56]. Subsequently, the substrate temperature was slowly increased again to 400°C in As_4 flux and a 310-ML-thick GaAs was grown at 400°C by the conventional growth method with a growth rate of 0.5 ML/s. The sample structure with a 100-nm GaAs capping layer is illustrated in Figure 3.12 (b).